Batteries & Supercaps

Research Article
doi.org/10.1002/batt.202400068

Chemistry Europe
European Chemical Societies Publishing

www.batteries-supercaps.org

Ionic Liquids as Cathode Additives for High Voltage Lithium Batteries

Matteo Palluzzi,[a] Akiko Tsurumaki,*[a, c] Nataliia Mozhzhukhina,[b] Josef Rizell,[b] Aleksandar Matic,[b] Paola D'Angelo,[a] and Maria Assunta Navarra*[a, c]

Two oxalatoborate ionic liquids (ILs), which are commonly utilized as electrolyte additives that form a protective layer on the cathode surface, are investigated for the first time as electrode additives. Cathodes based on $LiNi_{0.5}Mn_{1.5}O_4$ (LNMO) containing 3 wt% ILs, i.e., "IL-enriched cathodes", exhibit capacity values above 120 mAh/g with high Coulombic efficiencies throughout cycling over 200 times. A cathode without ILs also exhibits a capacity of 119 mAh/g but its Coulombic efficiency becomes low and unstable after 109 cycles. In addition, when 0.3 M ILs are added to conventional carbonate-based electrolytes, the battery cycle life improves but there is a reduction in the capacity probably due to low ionic conductivity of the electrolyte mixtures. Post-mortem analyses of electrodes retrieved from cycled cells highlight less electrolyte decomposition and less cathode corrosion, enabled by using the IL as the additive in LNMO, which are confirmed by a particle shape with smooth surface identical to the fresh cathode. The study demonstrates that oxalatoborate ILs can be used as the electrode additive, and this provides a new concept for cathode formulations for high performance batteries with a small amount of ILs.

Introduction

Since their introduction to the market by Sony in 1991, Li-ion batteries (LIBs) have become the dominant energy storage systems for portable electronic devices. The need for higher performance, especially higher energy density, is still increasing. To meet this demand, a shift from conventional cathode materials such as $LiCoO_2$, which operates at about 4 V vs. Li^+/Li, to new materials that can reach 5 V vs. Li^+/Li is necessary. A promising material in this respect is $LiNi_{0.5}Mn_{1.5}O_4$ (LNMO), which has a voltage plateau as high as 4.7 V vs. Li^+/Li, a notable specific capacity of 147 mAh/g, and no cobalt in its structure.

However, despite these attractive features, this material has not been used at a commercial scale due to a series of problems. First, the high voltage of the Ni^{4+}/Ni^{2+} redox processes leads to decompositions of conventional carbonate-based electrolytes on the cathode surface.[1–3] Second, even a small amount of water or impurities in the electrolyte reacts with $LiPF_6$, which is the most common lithium salt found in the electrolyte for LIBs, and produces HF, causing corrosion of the cathode and dissolution of Ni^{2+} and Mn^{2+}.[3,4] Third, depending on the synthesis procedures of LNMO, Mn^{3+} can be present in the structure,[1,4] which is prone to disproportionate to Mn^{2+} and Mn^{4+}, the former being extremely soluble in carbonate-based electrolytes.[1–4] Furthermore, when LNMO is not fully lithiated, it tends to self-discharge through electrolyte oxidation, which leads to further formation of HF and dissolution of Mn and Ni.[3,4] These phenomena become more evident at higher temperatures,[1,3] higher state of charge, and longer storage time.[3] Finally, Mn^{2+} and Ni^{2+} originating from the cathode can migrate to the anode side to be reduced, wasting Li^+ and deteriorating/destroying the solid electrolyte interphase (SEI),[1–4] undermining the performances of the battery.

The formation of a stable cathode electrolyte interface (CEI) has been recognized as a promising strategy to improve the capacity retention of LNMO.[1,5–8] In this manner, a direct contact between the electrolyte and the electrode is avoided, preventing the decomposition of electrolytes and formation of HF, in tune improving the interfacial stability.[9] The realization of a well-designed CEI, being a good Li^+-conductor and providing protection, has been one of the main focuses of research during recent years. To realize this goal, the most employed strategy is the addition of a co-solvent or salts as a sacrificial agent to electrolytes[8,9] or electrodes.[10] In the case of LNMO, a boron-rich CEI is known to be particularly suitable to suppress the side-reactions on cathode surface, and oxalatoborate salts, such as lithium bis(oxalato)borate (LiBOB) and lithium difluoro(oxalato)borate (LiDFOB), have been proposed as additives to carbonate-based electrolytes for LIBs.[11,12] The addition of these salts improves the capacity retention upon cycling of the cells. Ionic liquids (ILs) are also promising additives for the electrolytes,[13,14] which are thermally, chemically, and electro-

[a] M. Palluzzi, Dr. A. Tsurumaki, Prof. P. D'Angelo, Prof. M. A. Navarra
Department of Chemistry
Sapienza University of Rome
Piazzale Aldo Moro 5, 00185 Rome, Italy
E-mail: akiko.tsurumaki@uniroma1.it
mariassunta.navarra@uniroma1.it

[b] Dr. N. Mozhzhukhina, J. Rizell, Prof. A. Matic
Department of Physics
Chalmers University of Technology
41296 Göteborg, Sweden

[c] Dr. A. Tsurumaki, Prof. M. A. Navarra
Hydro-Eco Research Center
Sapienza University of Rome
Via A. Scarpa 16, 00161 Rome, Italy

Supporting information for this article is available on the WWW under https://doi.org/10.1002/batt.202400068

Research Article
doi.org/10.1002/batt.202400068
Chemistry Europe
European Chemical Societies Publishing

chemically stable, and those with oxalatoborate anions are used to support CEI formation.

In spite of promising features of ILs, it is important to consider the high cost and environmental impact of ILs, which counterweight their advantage from an economic point of view.[15–18] Considering that the most beneficial effects of ILs are exerted on the cathode surface through CEI formation, we propose in this study a selective distribution of the ILs on the LNMO cathode surface. Specifically, two oxalatoborate-based ILs: *N*-methyl-*N*-propylpiperidinium bis(oxalato)borate ($PIP_{1,3}BOB$) and *N*-methyl-*N*-propylpiperidinium difluoro(oxalato)borate ($PIP_{1,3}DFOB$), were synthesized and added to the cathode during its slurry formulation, realizing "IL-enriched cathodes", instead of adding ILs in the electrolyte. In the literature, there are only few reports on IL-addition to cathodes[19–23] and they are all devoted to the realization of solid-state batteries. To the best of our knowledge, this is the first attempt to use ILs as the cathode additive to boost the compatibility of high energy cathode materials with organic liquid electrolytes.

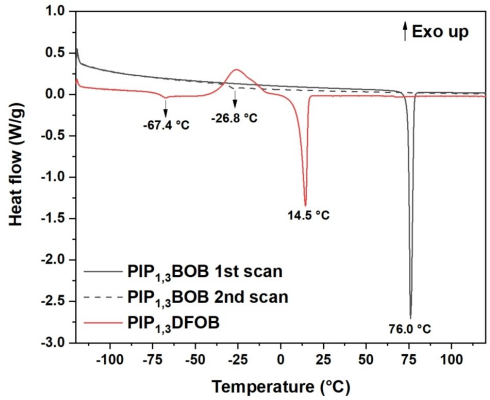

Figure 1. DSC curves of the two ILs.

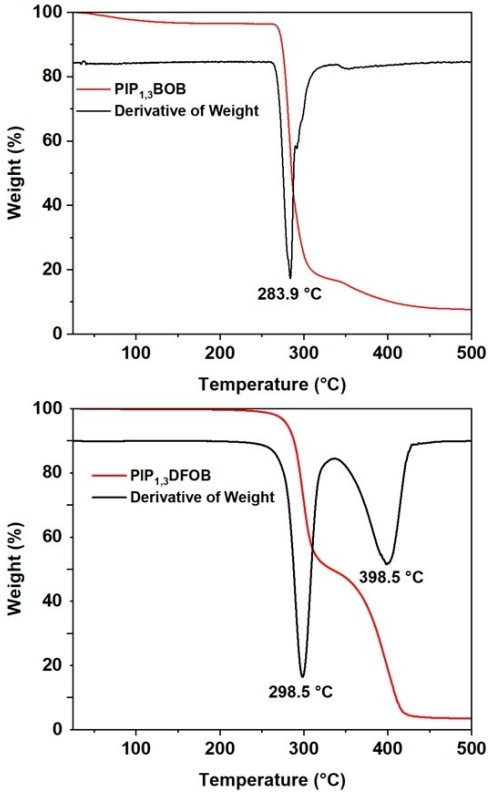

Figure 2. TGA (red line) and corresponding first derivative curves (black line) of the two ILs.

Results and Discussion

Thermal Properties of ILs

The thermal properties of the synthesized ILs have been characterized by DSC (Figure 1) and TGA (Figure 2). In the case of $PIP_{1,3}BOB$, which is a white powder at room temperature, a melting point was observed at 76.0 °C during the first scan, while it was not observed during the subsequent scan due to super-cooling.[5] In the second scan, a glass transition at −26.8 °C was instead observed. Regarding $PIP_{1,3}DFOB$, both the glass transition and melting points were observed in the first scan at −67.4 °C and 14.5 °C, respectively. A cold-crystallization was observed before the melting point, which is a common phenomenon for ILs.[6]

TGA highlighted the notable thermal stability of both ILs, making their use suitable for battery applications. More specifically, $PIP_{1,3}BOB$ has a single decomposition process at 283.9 °C while $PIP_{1,3}DFOB$ decomposes through a two-step process. The first step is at 298.5 °C, which can be attributed to the decomposition of the oxalatoborate moiety, while the second at 398.5 °C is attributable to that of the fluoroborate moiety according to the literature.[5] The residual weight is due to decomposition products containing mainly B_2O_3.[24] For $PIP_{1,3}BOB$, it was around 10% while for $PIP_{1,3}DFOB$, having only one oxalatoborate moiety, it was around 5%.

Galvanostatic Performances of IL-Enriched Electrolyte and Electrode

In the first step of our investigation, the two ILs were studied as additives to the electrolyte. Mixtures of 0.3 M $PIP_{1,3}BOB$ or $PIP_{1,3}DFOB$ in 1M $LiPF_6$ in ethylene carbonate and dimethyl carbonate 1:1 v/v (LP30) were prepared and tested in Li|| LNMO cells at 1 C for 200 cycles (Figure 3). Identical cells with neat LP30 were also evaluated as a reference. A notable improvement in terms of long-term Coulombic efficiency (CE) was observed when LP30 + IL mixtures were used (Figure 3a). In the figures, the results after cell failure, i.e., the cycle with CE less than 60%, are not shown. For example, the cell with pure LP30 showed a stable cycling with CEs of at least 99% at the beginning but from the 109th cycle, the cell exhibited noticeable instabilities, reaching CE of 37% at the 121st cycle. After this cycle, CEs were continuously irregular, and thus, the results after this cycle are not shown. The cell employing LP30 + $PIP_{1,3}DFOB$ electrolyte instead maintained a CE of at least 98%

Research Article
doi.org/10.1002/batt.202400068
Chemistry Europe
European Chemical Societies Publishing

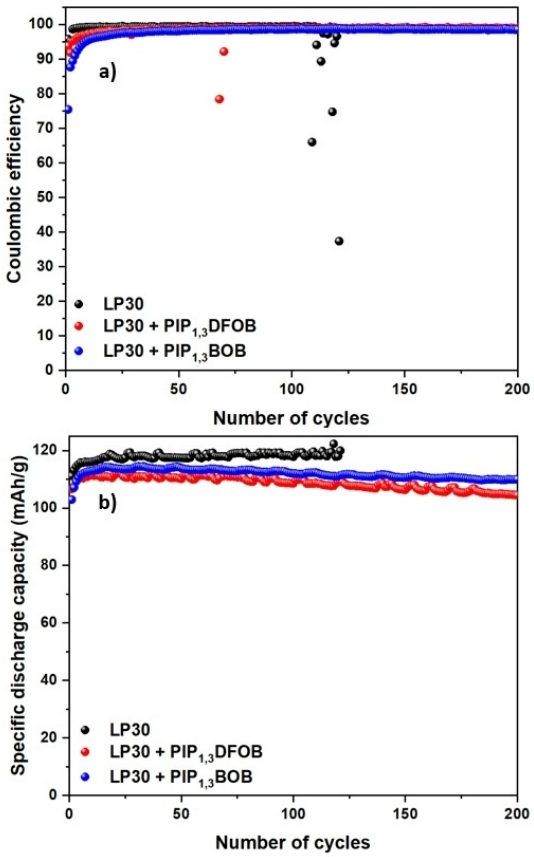

Figure 3. a) Coulombic efficiencies and b) specific discharge capacities of cells with LP30 + IL mixtures and LP30. The results after the cycle with a Coulombic efficiency below 60% are not shown.

over 200 cycles, with only two negligible CE drops at the 68th and 70th cycles which recovered already in their next cycles. Also, LP30 + $PIP_{1,3}BOB$ was able to keep CEs above 98% throughout the entire cycling.

On the other hand, regarding the specific capacity, Figure 3b shows that there is a slight loss of performances by replacing LP30 with LP30 + IL electrolytes, both in terms of discharge capacities and their retention. The maximum discharge capacity was 119 mAh/g for the cell with LP30, while it was 112 mAh/g and 115 mAh/g for the cells with LP30 + $PIP_{1,3}DFOB$ and LP30 + $PIP_{1,3}BOB$. The capacity retentions at the 100th cycle were found to be 98.7%, 96.7%, and 97.8%, respectively. The slightly lower capacity values for the cells with IL additives are probably due to the increased viscosity and slightly lower ionic conductivity of the electrolytes.[5] As the battery cycling continues, overpotential due to mass transport becomes pronounced, suggesting the larger resistance of CEI formed by the ILs (Figure S1), which in turn, should be the reason for long term battery function with high CEs. In contrast to this, the resistive but protective layer is considered not to grow in the case of neat LP30 without CEI constituents. This causes a series of side-reactions during cycling such as the dissolution of transition metals at the cathode side, which migrate towards the anode side and undermines the SEI.

Considering all the results together, it can be confirmed that the addition of ILs is effective for the formation of a protective layer on the LNMO surface. However, the presence of an excess ILs is not favourable in terms of ionic conductivity of the electrolyte, and it also causes continuous growth of CEI, increasing its resistivity. This is the reason behind the alternative use of the oxalatoborate ILs as cathode additives.

As the cathode additives, 3 wt% $PIP_{1,3}BOB$ and $PIP_{1,3}DFOB$ were added directly to the slurries during the electrode preparations to realize "BOB-enriched electrode" and "DFOB-enriched electrode", respectively. It should be emphasized that, considering an electrode with a mass load of 2.8 mg of active material, an addition of 3 wt% IL means that barely 0.1 mg of IL is present in a single cell. In contrast to this, when ILs are used as the additive to LP30, a cell with 60 μL of 0.3 M of $PIP_{1,3}BOB$ in LP30 contains 5.9 mg of the IL.

As shown in Figure 4a, there is an improvement in the cell stabilities by using IL-enriched electrodes compared to pristine LNMO electrodes. The DFOB-enriched electrode maintained a CE above 99% for 181 cycles, and even better results were obtained for the BOB-enriched electrode which was able to maintain a CE of at least 99% throughout 200 cycles without encountering any instability. Therefore, it is proved that the

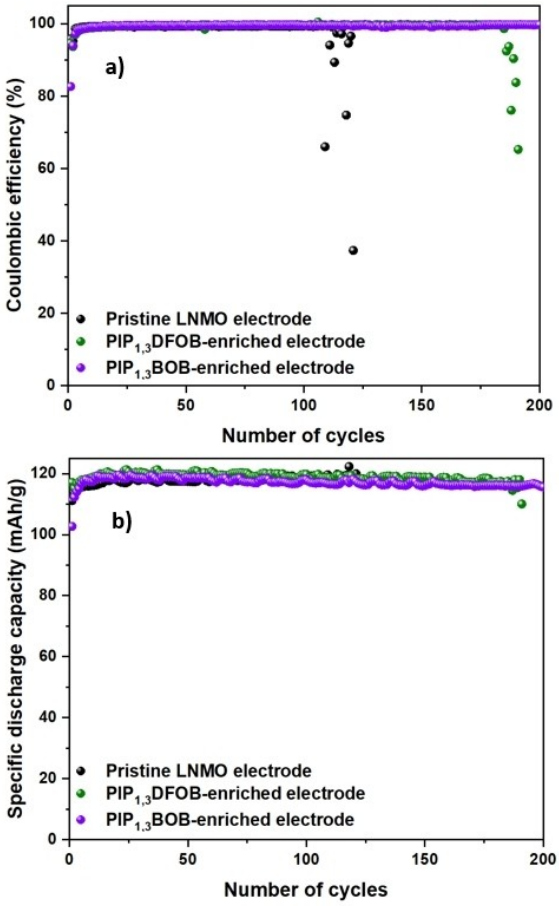

Figure 4. a) Coulombic efficiencies and b) specific discharge capacities of the IL-enriched electrodes. The results of pristine LNMO shown in Figure 3 are also shown here as a reference. The results after the cycle with the Coulombic efficiency below 60% are not shown.

Research Article
doi.org/10.1002/batt.202400068
Chemistry Europe
European Chemical Societies Publishing

stability improvement is possible even by adding a small amount of ILs directly in the electrodes. In addition, the cells with IL-enriched electrodes exhibited capacity values comparable or even superior to pristine LNMO electrodes (Figure 4b). The maximum discharge capacity was above 120 mAh/g for both the DFOB- and BOB- enriched electrodes.

Comparison between the "LP30 + IL mixture" approach and the "IL-enriched electrode" approach clarifies that there are similar stability improvements in both cases, while only the latter is able to maintain a higher capacity with a minimal capacity loss upon cycling. The combination of IL-enriched electrodes and pure LP30 is undoubtedly regarded as more advantageous than the combination between the pristine LNMO electrode and LP30 + IL mixture in terms of reduced amounts of ILs and improved performances.

The voltage profiles obtained from the IL-enriched electrodes and the reference LNMO electrode are reported in Figure 5. In all the profiles, both redox processes involving the Ni^{2+}/Ni^{4+} couple (at around 4.7 V vs. Li/Li^+) and the Mn^{3+}/Mn^{4+} couple (at around 4 V vs. Li/Li^+) are present. In the voltage profiles of the IL-enriched electrodes, it is possible to discern that the electrodes show a higher overpotential during the first cycle, which is probably caused by higher interfacial resistances due to the presence of the ILs on the surface of LNMO. Already at the fifth cycle, however, the overpotential disappears and voltage profiles become no longer different from those obtained using the pristine LNMO electrode. This can be caused by the dissolution of ILs in LP30, simultaneously with the CEI formation. Since there are larger irreversible capacities in the 1st charge when ILs are present, ILs are expected to be oxidized and consumed to form the CEI.

Impedance spectra were also recorded during the first ten cycles at a maximum state of charge to track changes in the resistances of the cell. Interfacial resistances were evaluated based on the diameter of semicircles of Nyquist plot, and their changes are reported in Figure S2. The IL-enriched electrodes exhibit higher interfacial resistances at the beginning as compared to the pristine LNMO. However, the interfacial resistances of all samples converged to 40–50 Ω after the 4th cycle. From impedance spectroscopy, it was not possible to confirm the formation of CEI. Thus, post-mortem analyses were carried out and are discussed in a following section.

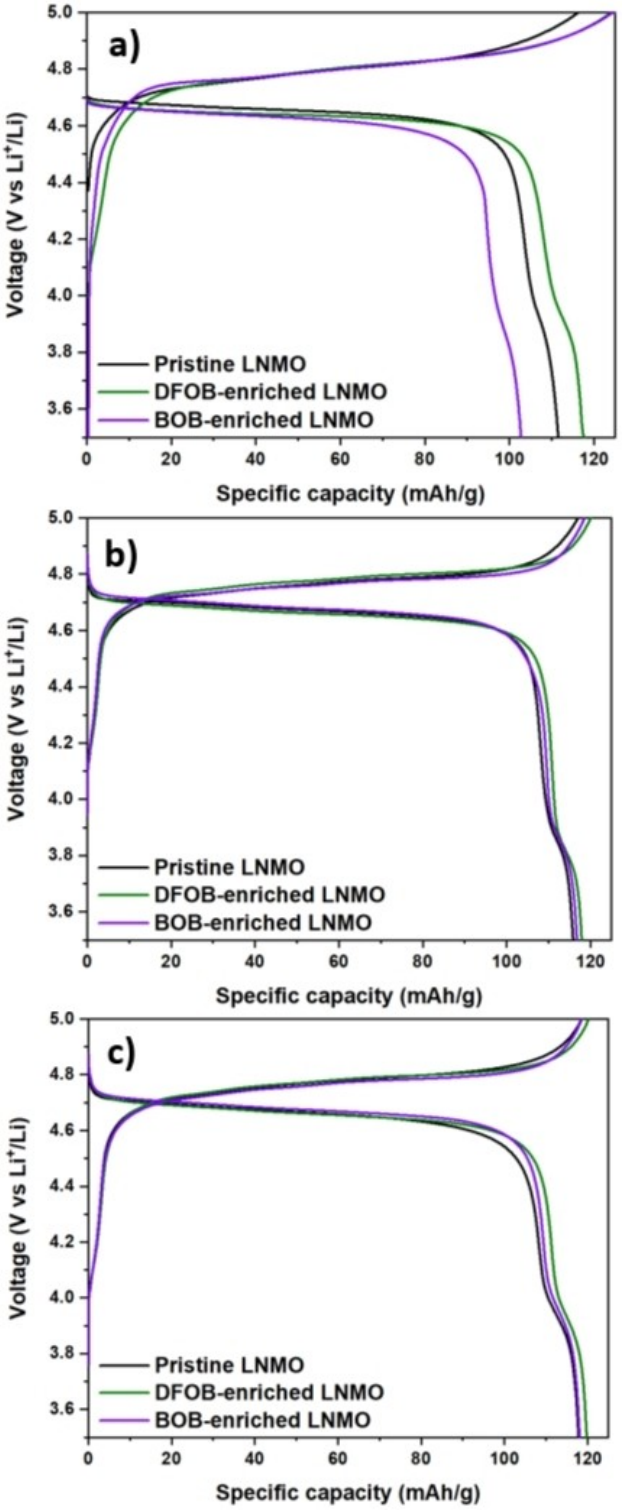

Figure 5. Voltage profile of Li||LNMO, Li||DFOB-enriched LNMO and Li||BOB-enriched LNMO cells. a) 1st cycle, b) 5th cycle, 100th cycle.

Electrochemical Properties of IL-Enriched Electrodes

As an intrinsic property of the electrodes, the Li^+ diffusion coefficient of LNMO during the intercalation/de-intercalation processes was evaluated through cyclic voltammetry at different scan rates performed on a Li||LNMO cell and a Li|| BOB-enriched LNMO cell with LP30 (reported in Figure S3a and Figure S3b). The measured maximum currents (in Amperes) were plotted against the square root of the scan-rates (in V/s) and linearly fitted (Figure S3c and Figure S3d). The slopes of the fitted lines were used to evaluate the Li^+ diffusion coefficient in these two cases according to the Randles-Sevcik equation (1):[25–27]

$$i = 268600 z^{3/2} A D^{1/2} C v^{1/2} \quad (1)$$

in which i is the maximum current measured (in A), v is the scan-rate (in V/s), A is the area of the electrode (0.785 cm^2 in the present case), C is the concentration of lithium in the

Research Article
doi.org/10.1002/batt.202400068
Chemistry Europe
European Chemical Societies Publishing

electrode (in mol cm^{-3}), z is the number of electrons exchanged during the intercalation/de-intercalation processes, and D is the diffusion coefficient expressed in cm^2/s. D values during intercalation (discharge) and de-intercalation (charge) were found to be 5.11×10^{-10} cm^2/s and 4.84×10^{-10} cm^2/s for pristine LNMO and 6.88×10^{-10} cm^2/s and 7.74×10^{-10} cm^2/s for BOB-enriched LNMO. Slightly higher values of the Li^+ diffusion coefficients were obtained during both intercalation and de-intercalation by adding ILs in LNMO. Given this slight difference in the intrinsic properties of LNMO electrodes with and without ILs, the improvement in battery performance likely depends on how degradation of battery components was suppressed during cycling.

Post-Mortem Characterizations

A series of post-mortem studies was performed using XPS, SEM and Raman spectroscopy on LNMO cathodes and BOB-enriched cathodes retrieved from cycled cells to detect how the presence of $PIP_{1,3}BOB$ improved the battery performances.

Figure 6 shows the SEM micrographs of the as-made and cycled LNMO and BOB-enriched LNMO electrodes. Compared to the uncycled pristine LNMO (Figure 6a), cycled LNMO (Figure 6b) shows a pronounced corrosion of the LNMO secondary particles, which is seen as irregular particle surfaces and blurred particle boundaries after cycling. This is expected to be a consequence of the formation of HF in the electrolyte,[3] causing the dissolution of transition metals from LNMO. On the other hand, for BOB-enriched electrodes, images before (Figure 6c) and after 200 cycles (Figure 6d) do not exhibit any sign of corrosion. These results suggest that a protective layer was formed on the LNMO surface, reducing the decomposition of the electrolyte and HF formation which damages the electrodes.

The degradation of the cathode was also visible in the Raman spectra (Figure 7). Both the as-made pristine LNMO (Figure 7a) and BOB-enriched LNMO (Figure 7c) electrodes show all the typical signals of the spinel structure as already reported in the literature.[28] However, the pristine sample (Figure 7b) loses all these features after cycling and shows only a large band centred at 556 cm^{-1} probably related to LiF, indicating an alternation of electrode surface. In the latter case (Figure 7d) instead, most of the features are preserved, showing only a widening and a lowering of the signals. These results suggest that the BOB-enriched electrode is more stable upon galvanostatic cycling.

From SEM and Raman spectroscopies, a better stability of BOB-enriched LNMO was confirmed. We believe that this is achieved by the formation of a protective layer on LNMO, i.e., CEI, which prevents the electrode damages by HF. In order to confirm this hypothesis, XPS measurements of a cycled LNMO electrode and BOB-enriched electrode were performed. The C1s (Figure 8a and Figure 8b) and O1s (Figure 8c and Figure 8d) regions of the spectra highlight a stronger intensity of the C–O and C=O peaks in the pristine LNMO, respectively. This suggests a suppressed decomposition of the electrolyte when a BOB-enriched electrode is employed. For the BOB-enriched electrode, when the ratio of C–O/C=O is compared between the C1s and O1s regions, it can be noticed that the ratio results to be slightly higher in the case of O1s region. This can be due to B–O bonds, whose signal appears in the same energy range of C–O. This suggests the formation of a CEI based on the anion of ILs. In the O1s spectrum also the M–O peak is visible at 530.2 eV, and its intensity is higher in the case of BOB-enriched electrode, suggesting that the surface of LNMO is more exposed. In the F1s spectra (Figure 8e and Figure 8f), the peak corresponding to LiF is weaker for BOB-enriched electrodes. The signal is due to a byproduct caused by the salt decomposition. Taking all results into account, the use of BOB-enriched electrodes is considered to lead to the formation of a CEI, including

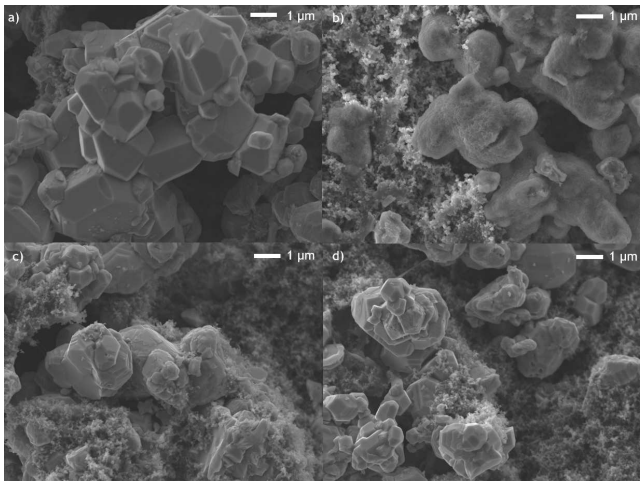

Figure 6. SEM micrographs of a) as-made pristine LNMO electrode, b) cycled pristine LNMO electrode, c) as-made BOB-enriched LNMO electrode, d) cycled BOB-enriched LNMO electrode. All the micrographs are recorded with a x10k magnification.

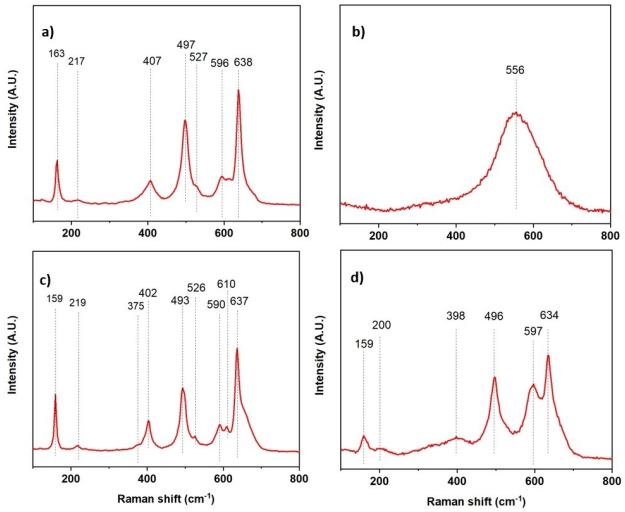

Figure 7. Raman spectra from a) as-made LNMO electrode, b) LNMO electrode after cycling, c) as-made BOB-enriched LNMO electrode, d) BOB-enriched LNMO electrode after cycling.

Research Article
doi.org/10.1002/batt.202400068
Chemistry Europe
European Chemical Societies Publishing

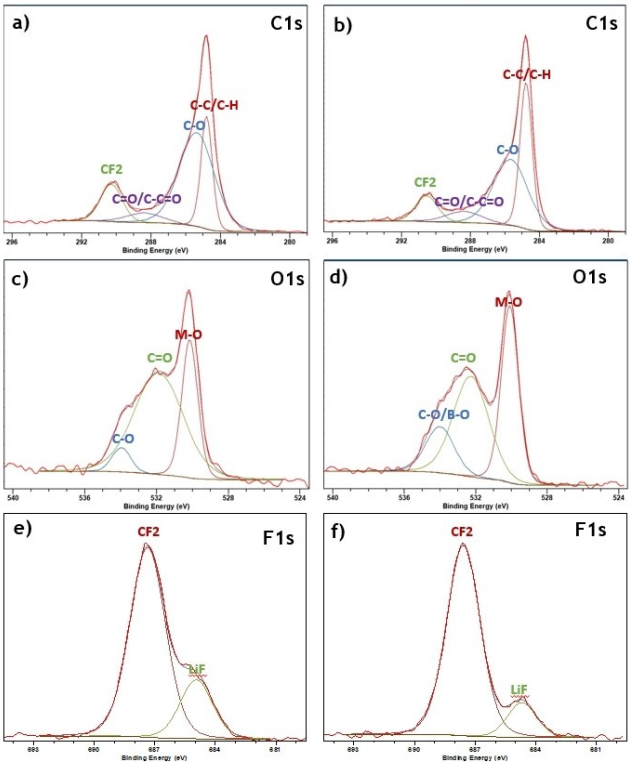

Figure 8. XPS of cycled electrodes. a) C1s, c) O1s, and e) F1s regions of pristine LNMO electrodes. b) C1s, d) O1s, and f) F1s regions of BOB-enriched LNMO electrodes.

B–O bonds and being thin enough not to completely cover the LNMO surface but enough to reduce the reaction with HF.

Conclusions

In this study two ILs, namely $PIP_{1,3}$DFOB and $PIP_{1,3}$BOB, were synthesized and used as additives to LNMO electrodes to produce "IL-enriched electrodes". These electrodes exhibited an outstanding stability over 200 cycles when cycled at 1 C in Li-metal cells in terms of Coulombic efficiency, a high specific capacity, and its retention, outperforming pristine LNMO which failed after 109 cycles. By adding the same ILs in LP30, i.e., using IL as the electrolyte additive, it was also possible to improve the battery cycle stability, but specific capacities were reduced probably due to the reduced ionic conductivity, suggesting that the use of these ILs to realize IL-enriched electrodes is more beneficial than their use to realize LP30 + IL mixtures. The amount of ILs in the cells assembled using the IL-enriched electrodes is about sixty times lower than the one in the cells with IL-electrolyte mixtures. Post-mortem analyses performed on the electrodes retrieved from cells confirmed that the use of IL-enriched electrodes leads to less corrosion of the LNMO particles and preservation of their surface structure. In conclusion, our results pave the way for new approaches to the use of ILs in the battery field that are potentially more beneficial in terms of the performance improved by a very small amount of ILs.

Supporting Information

All the details regarding the experimental procedures, the synthesis methods and additional results can be found in the Supplementary Information. The authors have cited additional references within the Supporting Information (Ref. [29]).

Acknowledgements

M.P. thanks Sapienza University of Rome for funding Progetto per Avvio alla Ricerca-Tipo 1 AR1221816B56 A67B, and for the financial support of PhD students' mobility abroad. M.A.N. thanks the financial support of the National Recovery and Resilience Plan (PNRR), Mission 4 Component 2 Investment 1.3, funded from the European Union – NextGenerationEU, within the Spoke 6 "Energy Storage" of the Extended Partnership (PE2) NEST – Network 4 Energy Sustainable Transition". The authors thank Martina Olsson for the support received during the acquisition of SEM images.

Conflict of Interests

The authors declare no conflict of interest.

Data Availability Statement

The data that support the findings of this study are available from the corresponding author upon reasonable request.

Keywords: ionic liquids · lithium · high-voltage cathodes · LNMO · cathode additives

[1] H. Zhao, W. A. Lam, L. Sheng, L. Wang, P. Bai, Y. Yang, D. Ren, H. Xu, X. He, *Adv. Energy Mater.* **2022**, *12* (16), 2103894.
[2] A. Jarry, S. Gottis, Y.-S. Yu, J. Roque-Rosell, C. Kim, J. Cabana, J. Kerr, R. Kostecki, *J. Am. Chem. Soc.* **2015**, *137* (10), 3533–3539.
[3] N. P. W. Pieczonka, Z. Liu, P. Lu, K. L. Olson, J. Moote, B. R. Powell, J.-H. Kim, *J. Phys. Chem. C* **2013**, *117* (31), 15947–15957.
[4] T.-F. Yi, J. Mei, Y.-R. Zhu, *J. Power Sources* **2016**, *316*, 85–105.
[5] A. Tsurumaki, M. Branchi, A. Rigano, R. Poiana, S. Panero, M. A. Navarra, *Electrochim. Acta* **2019**, *315*, 17–23.
[6] G. Di Donato, G. Maresca, M. Palluzzi, A. Tsurumaki, M. A. Navarra, *Materials* **2023**, *16* (4), 1411.
[7] E. R. Østli, A. Mathew, J. R. Tolchard, D. Brandell, A. M. Svensson, S. M. Selbach, N. P. Wagner, *Batter. Supercaps* **2023**, *6 (7)*, e202300085.
[8] F. Wu, A. Mullaliu, T. Diemant, D. Stepien, T. N. Parac-Vogt, J. Kim, D. Bresser, G. Kim, S. Passerini, *InfoMat* **2023**, *5* (8), e12462.
[9] X. Zhang, G. Liu, T. Jiao, Y. Zou, Q. Wu, X. Chen, Y. Yang, J. Zheng, *Energy Mater.* **2021**, *1*, 100005.
[10] X. Bian, Q. Pang, Y. Wei, D. Zhang, Y. Gao, G. Chen, *Chem. Eur. J.* **2018**, *24*, 13815–13820.
[11] S.-Y. Ha, J.-G. Han, Y.-M. Song, M.-J. Chun, S.-I. Han, W.-C. Shin, N.-S. Choi, *Electrochim. Acta* **2013**, *104*, 170–177.
[12] M. Hu, J. Wei, L. Xing, Z. Zhou, *J. Appl. Electrochem.* **2012**, *42*, 291–296.
[13] L. Lombardo, S. Brutti, M. A. Navarra, S. Panero, P. Reale, *J. Power Sources* **2013**, *227*, 8–14.
[14] J. R. Nair, F. Colò, A. Kazzazi, M. Moreno, D. Bresser, R. Lin, F. Bella, G. Meligrana, S. Fantini, E. Simonetti, G. B. Appetecchi, S. Passerini, C. Gerbaldi, *J. Power Sources* **2019**, *412*, 398–407.

[15] G. B. Appetecchi, S. Scaccia, C. Tizzani, F. Alessandrini, S. Passerini, *J. Electrochem. Soc.* **2006**, *153* (9), A1685.
[16] M. Montanino, F. Alessandrini, S. Passerini, G. B. Appetecchi, *Electrochim. Acta* **2013**, *96*, 124–133.
[17] S. Passerini, G. B. Appetecchi, *MRS Bull.* **2013**, *38* (7), 540–547.
[18] E. Simonetti, M. De Francesco, M. Bellusci, G. Kim, F. Wu, S. Passerini, G. B. Appetecchi, *ChemSusChem* **2019**, *12* (22), 4946–4952.
[19] L. Liu, X. Qi, Q. Ma, X. Rong, Y.-S. Hu, Z. Zhou, H. Li, X. Huang, L. Chen, *ACS Appl. Mater. Interfaces* **2016**, *8* (48), 32631–32636.
[20] Q. Zhang, K. Pan, M. Jia, X. Zhang, L. Zhang, H. Zhang, S. Zhang, *Electrochim. Acta* **2021**, *368*, 137593.
[21] D. Y. Oh, Y. J. Nam, K. H. Park, S. H. Jung, S. Cho, Y. K. Kim, Y. Lee, S. Lee, Y. S. Jung, *Adv. Energy Mater.* **2015**, *5* (22), 1500865.
[22] S. Kinoshita, K. Okuda, N. Machida, T. Shigematsu, *J. Power Sources* **2014**, *269*, 727–734.
[23] T. Zhang, H. A. Zhou, *Nat. Commun.* **2013**, *4* (1), 1817.
[24] K. Xu, S. Zhang, T. R. Jow, W. Xu, C. A. Angell, *Electrochem. Solid-State Lett.* **2002**, *5* (1), A26.
[25] M. M. Loghavi, A. Nahvibayani, M. H. Moghim, M. Babaiee, S. Baktashian, R. Eqra, *Monatsh. Chem.* **2022**, *153* (12), 1197–1212.
[26] A. Wei, J. Mu, R. He, X. Bai, Z. Liu, L. Zhang, Y. Wang, Z. Liu, *Ceram. Int.* **2021**, *47* (1), 226–237.
[27] S. Monaco, F. De Giorgio, L. Da Col, M. Riché, C. Arbizzani, M. Mastragostino, *J. Power Sources* **2015**, *278*, 733–740.
[28] P. Jehnichen, C. Korte, *Anal. Chem.* **2019**, *91* (13), 8054–8061.
[29] N. Fairley, V. Fernandez, M. Richard-Plouet, C. Guillot-Deudon, J. Walton, E. Smith, D. Flahaut, M. Greiner, M. Biesinger, S. Tougaard, D. Morgan, J. Baltrusaitis, *Appl. Surf. Sci. Adv.* **2021**, *5*, 100112.

Manuscript received: January 31, 2024
Revised manuscript received: April 16, 2024
Accepted manuscript online: May 3, 2024
Version of record online: June 14, 2024